

Intergrowth Structure of Zeolite Crystals as Determined by Optical and Fluorescence Microscopy of the Template-Removal Process**

Lukasz Karwacki, Eli Stavitski, Marianne H. F. Kox, Jan Kornatowski, and Bert M. Weckhuysen*

Dedicated to Süd-Chemie on the occasion of its 150th anniversary

Zeolites and zeotype materials represent one of the most important types of heterogeneous catalysts widely used in the refining and petrochemical industry.^[1–4] Although industrial zeolite-based catalysts contain mostly nano-to-micrometer-sized crystallites, larger zeolite single crystals with dimensions of hundreds of micrometers have proven to be indispensable as model materials for diffusion and reactivity studies.^[5–9] It was established that these crystals often have complex structures consisting of several intergrown subunits.^[10,11] The way in which the building blocks are interconnected may severely affect intracrystalline transport properties or even make certain parts of the zeolite crystal completely inaccessible for the reactant molecules.^[5] For example, the intergrowth structure of ZSM-5 crystals elucidated from electron diffraction, X-ray diffraction, and optical microscopy results has been discussed over the past 20 years.^[11–14] Recently, Lehmann et al. visualized subunits of AlPO₄-5 crystals by probing intracrystalline concentrations of absorbed methanol by interference microscopy.^[15]

The hydrothermal synthesis of zeolites calls for structure-directing agents, such as alkyl amines, to ensure their long-range highly ordered porous structure. These template molecules have to be removed from the channels for the crystalline materials to be used as either adsorbents or shape-selective catalysts. To accomplish this, zeolites are calcined after synthesis to remove the template and allow reactant molecules to enter the channel system. Thermal decomposi-

tion of template molecules in different molecular sieves has been studied extensively mainly by thermoanalytical techniques,^[16,17] mass spectrometry,^[18,19] and NMR spectroscopy.^[20] These methods are bulk techniques, which average information over the whole catalyst sample. In contrast, relatively few attempts have been made to investigate physicochemical processes that take place in a single zeolite particle in a space- and time-resolved manner. The predominant method of choice to study calcination processes is IR microscopy,^[21] which has limited spatial resolution.

Herein, a new method is presented for determining the intergrowth structure on the basis of *in situ* mapping of the template-removal process in individual zeolite crystals. The formation of light-absorbing and -emitting species during the heating process has been monitored by a combination of optical and confocal fluorescence microscopy. As the accessibility of the porous network in the subunits varies,^[15] the individual building blocks can be readily visualized by monitoring the template-removal process in time. This concept has been successfully applied to four different zeolite crystals: CrAPO-5 (AFI structure), SAPO-34 (CHA structure), SAPO-5 (AFI structure), and ZSM-5 (MFI structure).

As a first example, we discuss the template-removal processes in CrAPO-5 materials as observed with *in situ* optical microscopy. The crystals ($45 \times 25 \times 22 \mu\text{m}^3$) appear flawless under the bright-field illumination; however, microphotographs taken during the heating process show that the crystals darken as a result of coke formation. Surprisingly, this process resulted in a nonuniform color pattern (Figure 1a). First, darkening is observed on the hexagonal flat planes of the crystals at 640 K, and then on the side planes at 675 K. Further on the hexagonal faces clear up and only dark ring patterns remain. At the same time a darkening front on the side planes advances towards the central part as the temperature increases. As the heating continues, the crystals regain translucency, indicating the complete removal of the template molecules. Similar results were obtained when the crystals were calcined in an oxidative atmosphere, but clearly template decomposition took place in this case (see the Supporting Information).

Together with these *in situ* optical microscopy measurements, we recorded Raman spectra, which showed a strong fluorescence background when the zeolite crystals were heated. These results suggest the formation of fluorescent intermediates, which could be further investigated with *in situ* fluorescence microscopy. The use of fluorescence microscopy in the field of heterogeneous catalysis has been pioneered by

[*] L. Karwacki, Dr. E. Stavitski, M. H. F. Kox,
Prof. Dr. ir. B. M. Weckhuysen
Inorganic Chemistry and Catalysis Group
Department of Chemistry
Utrecht University
Sorbonnelaan 16, 3584 CA Utrecht (The Netherlands)
Fax: (+31) 30-251-1027
E-mail: b.m.weckhuysen@uu.nl
Dr. J. Kornatowski
Max-Planck-Institut für Kohlenforschung
45470 Mülheim an der Ruhr (Germany)
and
Faculty of Chemistry
Nicholas Copernicus University
87-100 Torun (Poland)

[**] We thank the Dutch National Science Foundation (NWO-CW VICI and TOP grants) and the Research School Combination Catalysis (NRSC-C) for financial support.

 Supporting information for this article is available on the WWW under <http://www.angewandte.org> or from the author.

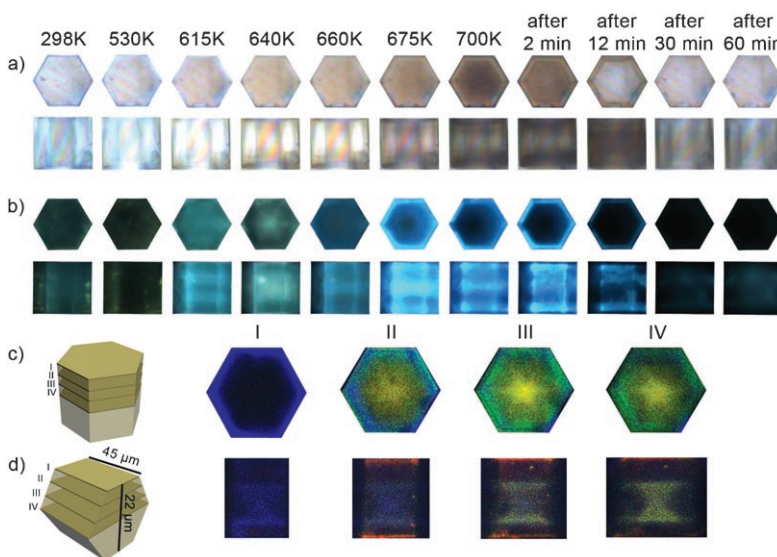


Figure 1. a) Optical microphotographs of CrAPO-5 taken during heating; b) Fluorescence microphotographs taken at the same temperatures as in (a); c,d) confocal fluorescence images of the CrAPO-5 crystals at 660 K. Confocal slices along the top and side planes are shown. Detection channels of 425–475, 510–550, and 575–635 nm are color-coded as blue, green, and red, respectively.

Roeffaers et al.^[8,22] We have, however, extended the range of experimental conditions in which this method can be applied by combining an upright fluorescence microscope with an in situ spectroscopic reaction cell, allowing studies in both the gas and liquid phase up to 900 K.^[23] Furthermore, by using the same in situ cell as for the optical microscopy measurements comparison of the data is possible. This combined optical and fluorescence approach will now be further explained.

Wide-field fluorescence microphotographs, taken during CrAPO-5 heating, are shown in Figure 1b. Strong fluorescence emerges at 615 K; as the heating continues, the features of the spatial pattern follow those observed with optical microscopy, with an exception of a starlike feature observable at 640 K. Besides wide-field fluorescence measurements, formation of fluorescent species within the zeolite crystal can be directly mapped in three dimensions by using confocal fluorescence microscopy, making possible an unequivocal visualization of the internal structure. Figure 1c and d shows optical slices taken along two different axes of the crystal at 660 K. The most intriguing features in this dataset are the six-pointed star (Figure 1c-III) and the hourglass patterns (Figure 1d-IV), which suggest an internal structure of the AFI crystal shown in Figure 2a. The intergrowth structure comprises two central hexagonal-pyramidal subunits and six smaller external blocks filling the void space. This model is in perfect agreement with the one deduced from the distribution of adsorbed methanol probed with interference microscopy.^[15] Along these lines, the hourglass pattern, observed at the relatively early stage of heating is due to the formation of fluorescent products in the inner subunits. The template is being removed from the outer section of the crystal at higher temperatures, which may be ascribed to the partial pore blockage at the interface of the subunits. The above observations are valid for about 90% of the studied CrAPO-5

crystals, but the longer crystals exhibit more complex color and fluorescence patterns, which is likely to be due to cleavage of the subunits.

The intergrowth structure of other zeolite crystals, such as SAPO-34, SAPO-5 and ZSM-5, could be revealed by the same combination of in situ optical and fluorescence microscopy. For example, rhombic SAPO-34 crystals feature a four-pointed star fluorescence pattern at 445 K, which is transformed into a square-shaped feature at 550 K (Figure 3a). Confocal optical slices at different temperatures show the cubic pattern, which advances from the exterior of the crystal inwards. This is illustrated in Figure 3b–d. The two observations are consistent with a model that involves six equal tetragonal-pyramidal-shaped subunits (Figure 2b).

In the third example, we investigated a series of SAPO-5 crystals varying in size. All the crystals demonstrate a similar fluorescence pattern upon heating (Figure 4). The findings lead to the proposal that SAPO-5 crystals

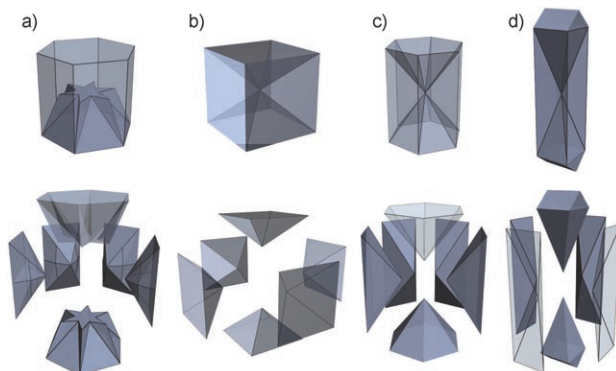


Figure 2. Normal and “exploded” representation of the proposed intergrowth structures of the zeolite crystals under study: a) CrAPO-5 (front subunits are not shown); b) SAPO-34; c) SAPO-5 (front subunits are not shown); d) ZSM-5.

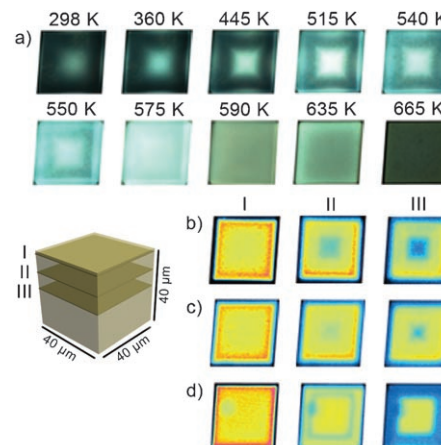


Figure 3. a) Fluorescence microphotographs of SAPO-34 taken during heating; b-d) confocal fluorescence images of SAPO-34 taken at 550 K, 575 K, and 635 K, respectively (561-nm laser, detection at 575–635 nm, false colors).

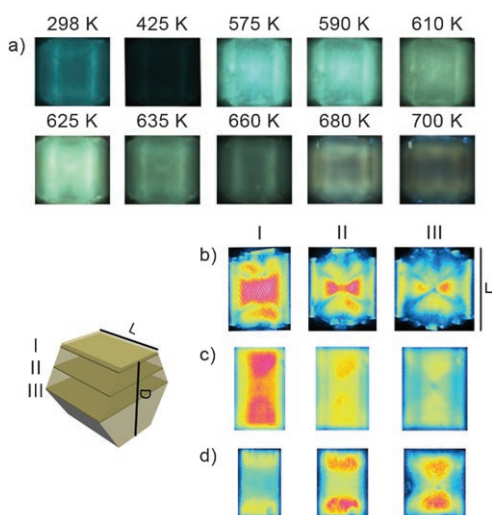


Figure 4. a) Fluorescence microphotographs of SAPO-5 taken during heating; b–d) confocal fluorescent images for three SAPO-5 crystals from different batches taken at 610 K (561-nm laser, detection at 575–635 nm, false colors). Average crystal sizes are b) $L=50\text{ }\mu\text{m}$, $D=50\text{ }\mu\text{m}$; c) $L=60\text{ }\mu\text{m}$, $D=35\text{ }\mu\text{m}$; d) $L=35\text{ }\mu\text{m}$, $D=20\text{ }\mu\text{m}$.

comprise two pyramidal-shaped subunits, meeting in a single spot at the center of the crystal (Figure 2c). As a final example, ZSM-5 crystals with dimensions of $50 \times 200 \times 50\text{ }\mu\text{m}^3$ were examined by the same approach. In this case, an hour-glass shape can be readily noticed in the wide-field fluorescence, confocal fluorescence images (Figure 5). Excellent

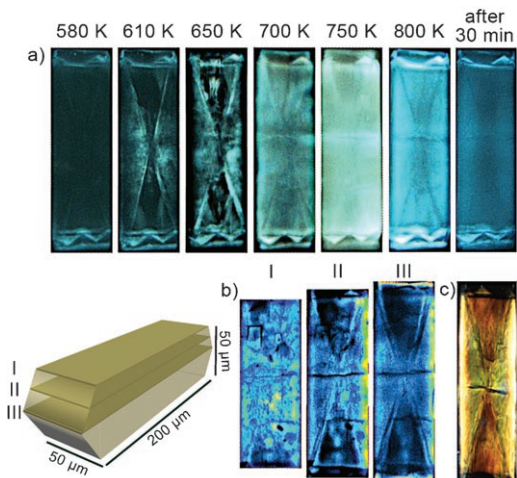


Figure 5. a) Fluorescence microphotographs of ZSM-5 crystals taken during template removal; b) confocal fluorescence images taken at 750 K. Detection channels are color-coded as in Figure 1; c) optical microphotograph taken at 800 K under crossed polarizers.

contrast can be also obtained in the present case in an optical microscopic image under crossed polarizers (Figure 5c) as described previously.^[24] The pattern is indicative of 90° intergrowths characteristic for large ZSM-5 crystals (Figure 2d).^[9,11,14,25]

By comparing the models depicted in Figure 2 one can notice a striking similarity between their building blocks. More specifically, the general model includes two pyramidal subunits, interconnected in the center of the zeolite crystal, surrounded by four or six building blocks. The observed commonality is in line with the assumption that the synthesis starts from rapid growth along one direction (usually crystallographic c axis), resulting in a dumbbell-shaped crystal, observed at the early stages of the synthesis.^[26] The gap around the center of the crystal is subsequently filled up to form a regular shape. It was proposed that a secondary nucleation process occurs at the interface between the central and outward structures, making the boundary between them defect-rich. These discontinuities in the crystalline structure and in the porous network are not sufficiently large to be directly noticeable by optical microscopy or SEM,^[27] but allow us to visualize the internal intergrowth structure.

Beyond determination of the intergrowth architecture of zeolite-type materials, the above observations also shed some light on the template-removal process. It was proposed that the removal of template molecules involves two distinct steps:^[16] at low temperature, the loosely bound template molecules, mostly a charged amines occupying the near-surface region, are driven away. As the temperature increases further, the template entrapped within the channels starts to decompose, mainly through a Hoffman elimination reaction, forming small fragments, which experience no steric obstacles to diffuse outward. Therefore, it is certainly of interest to elucidate the chemical nature of the fluorescence species formed during the heating process. As mentioned above, *in situ* Raman spectroscopy was shown to be inapplicable because the strong fluorescence background obscures the Raman signal. Apparently, the low concentration of the fluorescent intermediates also prevented their detection by separately conducted *in situ* IR microscopy experiments. However, the formation of light-absorbing and light-emitting species suggests that unsaturated products of the Hoffman reaction undergo side reactions in the zeolite channels, such as oligomerization. When diffusion is hindered by intergrowth boundaries, these oligomer chains are likely to grow longer or form conjugated aromatic compounds, leading to blackening of the crystal. An extreme example of such template carbonization process resulted in the formation of, for example, carbon nanotubes in zeolite channels.^[28]

In summary, we have shown that the decomposition of template molecules in zeolite-type crystals results in the formation of light-absorbing and fluorescent intermediates, and their spatial redistribution in the crystals during heating has been monitored for the first time by a combination of *in situ* optical and fluorescence microscopy. This generally applicable approach can now be used to elucidate the three-dimensional intergrowth structures of a wide range of catalytic important porous materials.

Received: May 7, 2007

Published online: August 31, 2007

Keywords: confocal microscopy · fluorescence · intergrowth · optical microscopy · template synthesis · zeolites

-
- [1] J. E. Naber, K. P. de Jong, W. H. J. Stork, H. Kuipers, M. F. M. Post, *Stud. Surf. Sci. Catal.* **1994**, *84*, 2197.
- [2] A. Corma, *Chem. Rev.* **1997**, *97*, 2373.
- [3] H. F. Rase, *Handbook of Commercial Catalysts: Heterogeneous Catalysts*, CRC, Boca Raton, FL, **2000**.
- [4] I. E. Maxwell, W. H. J. Stork, *Stud. Surf. Sci. Catal.* **2001**, *137*, 747.
- [5] G. Müller, T. Narbeshuber, G. Mirth, J. A. Lercher, *J. Phys. Chem.* **1994**, *98*, 7436.
- [6] Y. S. Lin, N. Yamamoto, Y. Choi, T. Yamaguchi, T. Okubo, S. I. Nakao, *Microporous Mesoporous Mater.* **2000**, *38*, 207.
- [7] J. Kärger, P. Kortunov, S. Vasenkov, L. Heinke, D. R. Shah, R. A. Rakoczy, Y. Traa, J. Weitkamp, *Angew. Chem.* **2006**, *118*, 8010; *Angew. Chem. Int. Ed.* **2006**, *45*, 7846.
- [8] M. B. J. Roeffaers, B. F. Sels, H. Uji-i, B. Blanpain, P. L'hoëst, P. A. Jacobs, F. C. De Schryver, J. Hofkens, D. E. De Vos, *Angew. Chem.* **2007**, *119*, 1736; *Angew. Chem. Int. Ed.* **2007**, *46*, 1706.
- [9] M. H. F. Kox, E. Stavitski, B. M. Weckhuysen, *Angew. Chem.* **2007**, *119*, 3726; *Angew. Chem. Int. Ed.* **2007**, *46*, 3652.
- [10] M. W. Anderson, K. S. Pachis, F. Prebin, S. W. Carr, O. Terasaki, T. Ohsuna, V. Alfreddson, *J. Chem. Soc. Chem. Commun.* **1991**, *1660*.
- [11] D. G. Hay, H. Jaeger, K. G. Wilshier, *Zeolites* **1990**, *10*, 571.
- [12] C. Weidenthaler, R. X. Fischer, R. D. Shannon, O. Medenbach, *J. Phys. Chem.* **1994**, *98*, 12687.
- [13] E. R. Geus, J. C. Jansen, H. van Bekkum, *Zeolites* **1994**, *14*, 82.
- [14] M. Kocirik, J. Kornatowski, V. Masarik, P. Novak, A. Zikanova, J. Maixner, *Microporous Mesoporous Mater.* **1998**, *23*, 295.
- [15] E. Lehmann, C. Chmelik, H. Scheidt, S. Vasenkov, B. Staudte, J. Karger, F. Kremer, G. Zadrozna, J. Kornatowski, *J. Am. Chem. Soc.* **2002**, *124*, 8690.
- [16] V. R. Choudhary, S. D. Sansare, *J. Therm. Anal.* **1987**, *32*, 777.
- [17] J. Kornatowski, G. Finger, D. Schultze, *J. Phys. Chem. A* **2002**, *106*, 3975.
- [18] J. P. Zhai, Z. K. Tang, F. L. Y. Lam, X. J. Hu, *J. Phys. Chem. B* **2006**, *110*, 19285.
- [19] X. T. Gao, C. Y. Yeh, P. Angevine, *Microporous Mesoporous Mater.* **2004**, *70*, 27.
- [20] P. Fejes, J. B. Nagy, J. Halasz, A. Oszko, *Appl. Catal. A* **1998**, *175*, 89.
- [21] M. Nowotny, J. A. Lercher, H. Kessler, *Zeolites* **1991**, *11*, 454.
- [22] M. B. J. Roeffaers, B. F. Sels, H. Uji-i, F. C. De Schryver, P. A. Jacobs, D. E. De Vos, J. Hofkens, *Nature* **2006**, *439*, 572.
- [23] E. Stavitski, M. H. F. Kox, B. M. Weckhuysen, *Chem. Eur. J.* **2007**, *13*, 7057.
- [24] C. Weidenthaler, R. X. Fischerand, R. D. Shannon and O. Medenbach, *J. Phys. Chem.* **1994**, *98*, 12687.
- [25] G. D. Price, J. J. Pluth, J. V. Smith, J. M. Bennett, R. L. Patton, *J. Am. Chem. Soc.* **1982**, *104*, 5971.
- [26] G. J. Klap, M. Wubbenhorst, J. C. Jansen, H. van Koningsveld, H. van Bekkum, J. van Turnhout, *Chem. Mater.* **1999**, *11*, 3497.
- [27] L. Brabec, M. Kocirik, *Mater. Chem. Phys.* **2007**, *102*, 67.
- [28] N. Wang, Z. K. Tang, G. D. Li, J. S. Chen, *Nature* **2000**, *408*, 50.